GAMMA-RAY PRODUCTION FROM COSMIC PROTON-ANTIPROTON INTERACTIONS

3-1 INTRODUCTION

A topic of importance to both cosmology and particle physics is the existence or nonexistence of antimatter in the universe (Alfvén, 1965). It is therefore of interest to determine the extent to which γ-ray astronomy may be useful in determining the existence of cosmologically distributed antimatter and antimatter sources in which matter-antimatter interactions take place.

For the purpose of discussion, we define the terms "RG" and "CR" as follows. An RG (rest-gas) proton (or antiproton) is one possessing negligible kinetic energy with respect to the surrounding gas in an astronomical system. For example, nuclei of the galactic interstellar gas clouds from which stars are formed may be considered RG nuclei. A CR (cosmic-ray) proton (or antiproton) would be one possessing relativistic energy. We may thus envision four situations for discussion in which matter and antimatter might interact:

(1) RG matter + RG antimatter (RG–$\overline{\text{RG}}$)
(2) RG matter + CR antimatter (RG–$\overline{\text{CR}}$)
(3) CR matter + RG antimatter (CR–$\overline{\text{RG}}$)
(4) CR matter + CR antimatter (CR–$\overline{\text{CR}}$)

Although astrophysics has revealed many surprising phenomena, we would be hard put to imagine a system in which the number of RG nuclei did not greatly outnumber the number of CR nuclei. Indeed, the evolution of such a system from a more balanced one would violate the second law of thermodynamics. Therefore, if we let the number of RG nuclei in a typical system be N and the number of CR nuclei in the system be of the order ϵN, with $\epsilon \ll 1$, then typical interaction rates would have the properties

$$\frac{R(\text{RG}-\overline{\text{CR}})}{R(\text{RG}-\overline{\text{RG}})} \sim \frac{R(\text{CR}-\overline{\text{RG}})}{R(\text{RG}-\overline{\text{RG}})} \sim \epsilon \qquad (3\text{-}1)$$

$$\frac{R(\mathrm{CR}-\overline{\mathrm{CR}})}{R(\mathrm{CR}-\overline{\mathrm{RG}})} \sim \frac{R(\mathrm{CR}-\overline{\mathrm{CR}})}{R(\mathrm{RG}-\overline{\mathrm{CR}})} \sim \epsilon \tag{3-2}$$

and

$$\frac{R(\mathrm{CR}-\overline{\mathrm{CR}})}{R(\mathrm{RG}-\overline{\mathrm{RG}})} \sim \epsilon^2 \tag{3-3}$$

We will thus assume that the likelihood of CR–$\overline{\mathrm{CR}}$ interactions is negligible compared to the likelihood of RG–$\overline{\mathrm{CR}}$ or CR–$\overline{\mathrm{RG}}$ interactions that will produce γ-rays of similar characteristics, and we may limit ourselves to the discussion of RG–$\overline{\mathrm{RG}}$ and RG–$\overline{\mathrm{CR}}$ (or CR–$\overline{\mathrm{RG}}$) interactions.

3-2 THE GAMMA-RAY SOURCE SPECTRUM

The γ-ray source spectrum from p–$\bar{p}$ interactions of the RG–$\overline{\mathrm{CR}}$ type is given by (cf. eqs. (1–10) through (1–14))

$$q_{\mathrm{RG}-\overline{\mathrm{CR}}}(E_\gamma) = 4\pi n_p(\mathbf{r}) \int dE_{\bar{p}} I(E_{\bar{p}}, \mathbf{r}) \sum_s \int dE_s \sigma_s(E_s|E_{\bar{p}}) \times \sum_d \zeta_{\gamma d} R_{\gamma d} f_{ds}(E_\gamma|E_s) \tag{3-4}$$

For interactions of the CR–$\overline{\mathrm{RG}}$ type, we use the corresponding expression

$$q_{\mathrm{CR}-\overline{\mathrm{RG}}}(E_\gamma) = 4\pi n_{\bar{p}}(\mathbf{r}) \int dE_p I(E_p, \mathbf{r}) \sum_s \int dE_s \sigma_s(E_s|E_p) \times \sum_d \zeta_{\gamma d} R_{\gamma d} f_{ds}(E_\gamma|E_s) \tag{3-5}$$

The notation for equations (3–4) and (3–5) is the same as that used in chapter 1. The quantity $n(\mathbf{r})$ is the number of target nucleons in the medium per cubic centimeter as a function of position; $I(E, \mathbf{r})$ is the differential cosmic-ray particle flux in $\mathrm{cm^{-2}\text{-}s^{-1}\text{-}sr^{-1}\text{-}GeV^{-1}}$. The subscript p stands for proton, $\bar{p}$ for antiproton, s for secondary particle produced in the collision, and d for decay mode. The production function $\sigma_s(E_s|E_p)$ represents the cross section for production of secondary particles of type s and energy E_s in a collision of primary energy E_p, $\zeta_{\gamma d}$ represents the number of γ-rays produced in the decay mode d, $R_{\gamma d}$ is the branching ratio for the decay mode d (the probability that a secondary particle s will decay via mode d) and $f_{ds}(E_\gamma|E_s)$ is the normalized distribution function representing the probability that a secondary

particle with energy E_s will decay to produce a γ-ray of energy E_γ. For the purposes of discussion, we will restrict ourselves to $p-\bar{p}$ interactions.

The situation for matter-antimatter annihilations occurring near rest is somewhat different. In this case, we will find it more convenient to speak of particle densities instead of fluxes or intensities. We thus make the transformation

$$\int dE_k I_k(E_k, \mathbf{r}) \rightarrow \frac{n_k(\mathbf{r})}{4\pi} \int dv\, v f(v) = \frac{n_k(\mathbf{r})\langle v \rangle}{4\pi} \tag{3-6}$$

where v is the relative velocity between the annihilating nucleon and antinucleon, which we can consider to be a thermal velocity, and $f(v)$ is a normalized distribution function representing the distribution of relative velocities between the interacting nucleons.

The γ-ray source spectrum from $p-\bar{p}$ interactions at or near rest is given by

$$q_{\mathrm{RG}-\overline{\mathrm{RG}}}(E_\gamma) = n_p(\mathbf{r}) n_{\bar{p}}(\mathbf{r}) \int dv f(v) v \sum_s \int dE_s \sigma_s(E_s|v) \times \sum_d \zeta_{\gamma d} R_{\gamma d} f_{ds}(E_\gamma|E_s) \tag{3-7}$$

The form of equation (3–7) suggests that the introduction of the term "emission measure" be defined in analogy with its use in astrophysics (Shklovskii, 1960).

We therefore define the "emission measure" B as

$$B = \int dr n_p(\mathbf{r}) n_{\bar{p}}(\mathbf{r}) \tag{3-8}$$

It follows from equation (3–7) that

$$I_{\mathrm{RG}-\overline{\mathrm{RG}}}(E_\gamma) = \frac{1}{4\pi} \int dr q(\mathbf{r}) \alpha B \tag{3-9}$$

3–3 CROSS SECTIONS FOR PROTON-ANTIPROTON ANNIHILATIONS NEAR REST

We now state more precisely what we mean by a "rest gas." We define a rest gas to be a gas of particles such that no particle in the gas has an energy greater than 286 MeV. This rather liberal definition of rest is sufficient to insure that the only secondary particles produced in RG–$\overline{\mathrm{RG}}$ interactions that yield γ-rays are secondary mesons produced by nucleon-

antinucleon annihilation. Our restriction leaves out interactions of the type

$$p + \bar{p} \rightarrow p + \bar{p} + \pi^0 \tag{3-10}$$

since the threshold for reactions of this type is 286 MeV. (See ch. 1.)

Since the threshold for nonannihilation, inelastic, p–$\bar{p}$ interactions that produce particles other than π^0-mesons is even greater, it follows that in the RG–$\overline{\text{RG}}$ case, only annihilations; i.e., reactions of the form

$$p + \bar{p} \rightarrow \text{bosons} \hookrightarrow \text{neutral pions} \hookrightarrow \gamma\text{-rays} \tag{3-11}$$

need be considered.

Table 3–1 lists the experimental cross sections for free p–$\bar{p}$ annihilation as a function of incident antiproton kinetic energy at accelerator energies. Also listed are β_{cms} and the product of the annihilation cross section (σ_A) and cms velocity (β_{cms}). It can be seen from table 3–1 that the product of cms velocity and annihilation cross section is constant over a very large energy range. For nonrelativistic energies,

$$\beta_{\text{cms}} \simeq \tfrac{1}{2}\beta \qquad (\beta \ll 1) \tag{3-12}$$

β being the relative velocity of the particles. We find experimentally that

$$\sigma_A \simeq \frac{4.8 \times 10^{-26}\ \text{cm}^2}{\beta} \simeq \frac{1.4 \times 10^{-15}\ \text{cm}^3\text{-s}^{-1}}{v} \tag{3-13}$$

TABLE 3–1.—*Experimental Cross Sections for* p–$\bar{\text{p}}$ *Annihilation as a Function of Incident Antiproton Kinetic Energy*

$T_{\bar{p}}$, MeV	σ_A, mb	$\beta_{\bar{p}}$, cms	$\beta_{\bar{p}}\sigma_A$, mb	Reference
25 to 40	192 ±34	0.13	25	Loken and Derrick (1963).
45	175 ±45	.15	26	Cork et al. (1962).
40 to 55	155 ±27	.16	25	Loken and Derrick (1963).
55 to 80	118 ±26	.20	24	Loken and Derrick (1963).
90	101 ± 9	.22	22	Cork et al. (1962).
145	99 ± 8	.28	28	Cork et al. (1962).
245	66 ± 6	.36	24	Cork et al. (1962).
7000	23.6 ± 3.4	~1	24	Ferbel et al. (1965).

At all energies above 25 MeV, we find that table 3–1 agrees with the theoretical cross section

$$\sigma_A = \frac{\pi r_p^2}{\beta_{\text{cms}}} \tag{3–14}$$

taking

$$r_p = 0.87 \times 10^{-13} \text{ cm} \tag{3–15}$$

as the proton (or antiproton) radius and using the model of Koba and Takeda (1958) in which the nucleon acts as a black absorbing sphere of radius r_p.

At lower energies ($\lesssim 10$ MeV, which correspond to annihilations of matter and antimatter gases at a temperature $\lesssim 10^{11}$ K), coulomb forces play a dominant role in the matter-antimatter interaction process. At energies $\lesssim$ 100 eV, bound systems of protons and antiprotons can be formed as an intermediate stage before annihilation. The situation is similar to the case of positronium formation discussed in the last chapter. As was the case there, we find that under astrophysical conditions, the lifetime of the p–$\bar{p}$ system against annihilation is much shorter than its lifetime against breakup, so that the cross section for bound-state formation becomes the effective annihilation cross section. Until recently the effect of coulomb interactions on matter-antimatter annihilation was largely neglected and theoretical cross sections for bound-state formation processes had not been calculated. However, recently Morgan and Hughes (1970) have calculated the cross sections for the radiative capture processes

$$e^- + e^+ \rightarrow \Pi_e + \gamma \tag{3–16}$$

and

$$p + \bar{p} \rightarrow \Pi_p + \gamma \tag{3–17}$$

and the atomic processes

$$\bar{\text{H}} + \text{H} \rightarrow \Pi_p + (\Pi_e \text{ or } e^- + e^+) \tag{3–18}$$

$$\text{H}_2 + \text{H} \rightarrow \Pi_p + (\Pi_e \text{ or } e^- + e^+) + (\text{H or } p + e^-) \tag{3–19}$$

$$\text{H}_2 + \bar{\text{H}}_2 \rightarrow 2\Pi_p + (\text{various combinations of } 2e^-, 2e^+) \tag{3–20}$$

$$\text{H}_2 + \bar{\text{H}}_2 \rightarrow \Pi_p + (\Pi_e \text{ or } e^+ + e^-) + (\text{various combinations of } p, \bar{p}, e^+, \text{ and } 1e^-) \tag{3–21}$$

$$p + \bar{\text{H}} \rightarrow \Pi_p + e^+ \tag{3–22}$$

$$p + \bar{\text{H}}_2 \rightarrow \Pi_p + (\Pi_e \text{ or } e^+ + e^-) + (\bar{\text{H}} \text{ or } \bar{p} + e^+) \tag{3–23}$$

$$e^- + \bar{H} \rightarrow \Pi_e + \bar{p} \tag{3-24}$$

and

$$e^+ + H \rightarrow \Pi_e + p \tag{3-25}$$

where we have used the symbols Π_p and Π_e to denote the bound states of the $p-\bar{p}$ and $e^- - e^+$ systems, respectively. Reactions (3–24) and (3–25) have already been discussed in the previous chapter with regard to the annihilation of secondary cosmic-ray positrons in a tenuous neutral hydrogen gas. The cross sections for these reactions, as calculated by Cheshire (1964), will be given in a later chapter. With regard to $p-\bar{p}$ annihilation in intergalactic space, three processes in particular can be expected to be of the greatest importance:

(1) Direct annihilations, such as (3–11), at energies greater than 10 MeV, where the cross section can be well represented by equations (3–14) and (3–15).

(2) Direct annihilations at energies below 10 MeV, where the mutual coulomb attraction of the proton and antiproton distort the wave functions of the two particles with a resultant increase in the direct-annihilation cross section. When the cross section given by equation (3–14) is corrected for this effect, the cross-section formula becomes modified to

$$\sigma_A = \frac{2\pi\alpha/\beta}{1-\exp(-2\pi\alpha/\beta)} \frac{\pi r_p^2}{\beta_{\text{cms}}} \tag{3-26}$$

where α is the fine structure constant. For $p-\bar{p}$ interactions at energies much less than 4 MeV, where $\beta \ll 2\pi\alpha$, equation (3–26) reduces to

$$\sigma_A \simeq \frac{4\pi^2\alpha r_p^2}{\beta^2} \qquad \beta \ll 2\pi\alpha \tag{3-27}$$

Thus, at an energy of about 4 MeV, there is a transition in the velocity dependence of the annihilation cross section from $\sigma_A \sim \beta^{-1}$ to $\sigma_A \sim \beta^{-2}$. The same is true for electron-positron interactions at energies of the order of 2 keV where $\beta \approx 2\pi\alpha$.

(3) In interactions between neutral atomic gases of hydrogen and antihydrogen at thermal energies, the $H-\bar{H}$ rearrangement collision, reaction (3–18), becomes the dominant mode of $p-\bar{p}$ annihilation.

Morgan and Hughes (1970) have calculated the annihilation cross section for this reaction and found that, to within 20 percent for energies between 10^{-3} and 1 eV (corresponding to thermal velocities at temperatures between 10 K and 10^4 K)

$$\sigma_{\mathrm{H-H},A} \simeq (0.31 a_0^2)\beta^{-0.64} \tag{3-28}$$

where a_0 is the Bohr radius of the hydrogen atom.

Radiative capture reactions of the form of equation (3–17) can be shown to be insignificant. The cross section for annihilations of this type (Morgan and Hughes, 1970) is

$$\sigma_{A,r} = \frac{128}{3\sqrt{3}}\alpha\left(\frac{m_e}{m_p}\right)^2\left[\ln\left(\frac{\alpha}{\beta}\right) + 0.20 + 0.25\left(\frac{\alpha}{\beta}\right)^{-2/3}\right]\frac{\sigma_0}{\beta^2} \tag{3-29}$$

Equation (3–29) is accurate to within at least 1 percent when $\beta \leqslant \alpha/7$ and is exact in the limit as $\beta \to 0$. The radiative capture cross section for the electron-positron system, viz, $e^+ + e^- \to \Pi_e + \gamma$, is given by the same formula without the quantity $(m_e/m_p)^2$. For p–$\bar{p}$ annihilations at all energies of interest $\sigma_{A,r} \ll \sigma_A$; however, in the case of electron-positron annihilation (in an ionized medium) $\sigma_{A,r} > \sigma_A$ for interactions at energies less than 20 eV.

In figure 3–1 we give the cross section versus temperature, energy, and thermal velocity for the reactions expected to be of importance for cosmological problems (intergalactic p–$\bar{p}$ annihilations). Figure 3–2 shows the values for total-annihilation cross section times velocity (proportional to the annihilation rate) calculated by Morgan and Hughes, which should be valid for astrophysical and cosmological problems at the temperatures and kinetic energies indicated.

We may now make use of equations (3–17), (3–18), (3–27), and (3–28) in order to reduce equation (3–7) to a simpler form. To do this, let us assume that matter-antimatter annihilations are taking place at thermal energies in three temperature regions defined as

Region I:	$10^{11}\ \mathrm{K} \lesssim T \lesssim 10^{13}\ \mathrm{K}$	
Region II:	$10^4\ \mathrm{K} \lesssim T \lesssim 10^{11}\ \mathrm{K}$	(3–30)
Region III:	$10\ \mathrm{K} \lesssim T \lesssim 10^4\ \mathrm{K}$	

It follows from the equations cited above that in each of these regions the annihilation cross section varies as some inverse power of the veloc-

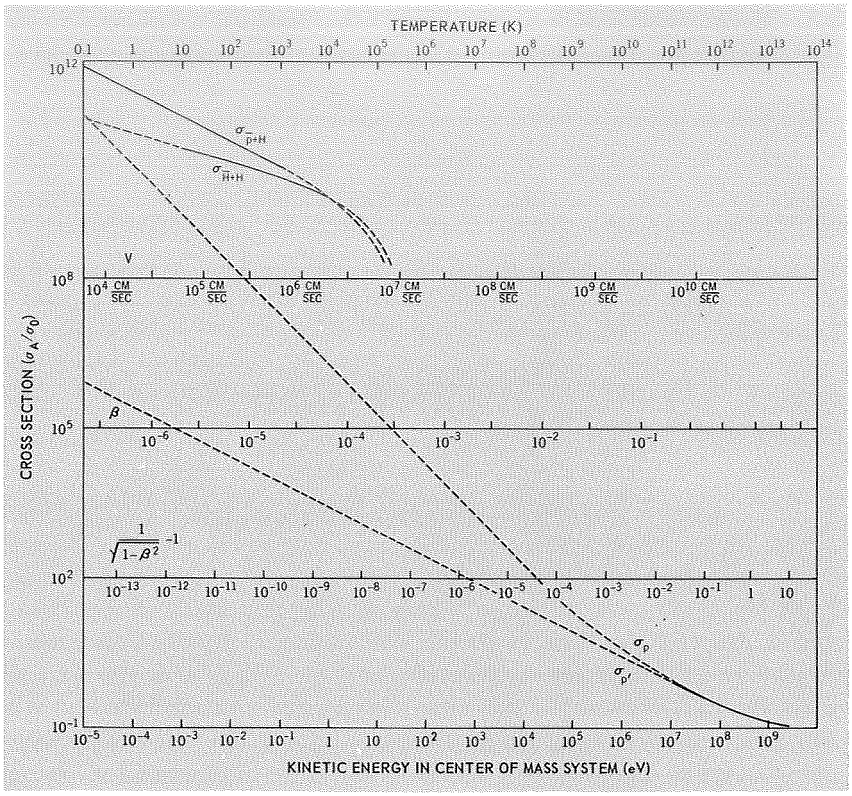

FIGURE 3–1.—Proton-antiproton annihilation cross sections as a function of temperature and kinetic energy for free nucleons and atoms (Morgan and Hughes, 1970). The curve marked σ_ρ takes into account the mutual coulomb attraction between the proton and antiproton; the curve marked $\sigma_{\rho'}$ is an extrapolation from the accelerator data that fails to take this effect into account.

ity. We can write an expression for this cross section for each of the temperature regions defined above thus

$$\begin{aligned}
&\text{Region I:} && \sigma(E_s|v) \simeq \sigma_{\mathrm{I}} \left(\frac{v}{c}\right)^{-1} \\
&\text{Region II:} && \sigma(E_s|v) \simeq \sigma_{\mathrm{II}} \left(\frac{v}{c}\right)^{-2} \qquad (3\text{–}31) \\
&\text{Region III:} && \sigma(E_s|v) \simeq \sigma_{\mathrm{III}} \left(\frac{v}{c}\right)^{-0.64}
\end{aligned}$$

where

$$\sigma_{\mathrm{I}} = 4.8 \times 10^{-26} \text{ cm}^2$$

and

$$\begin{aligned}
\sigma_{\mathrm{II}} &= 2.2 \times 10^{-27} \text{ cm}^2 \qquad (3\text{–}32) \\
\sigma_{\mathrm{III}} &= 2.6 \times 10^{-18} \text{ cm}^2
\end{aligned}$$

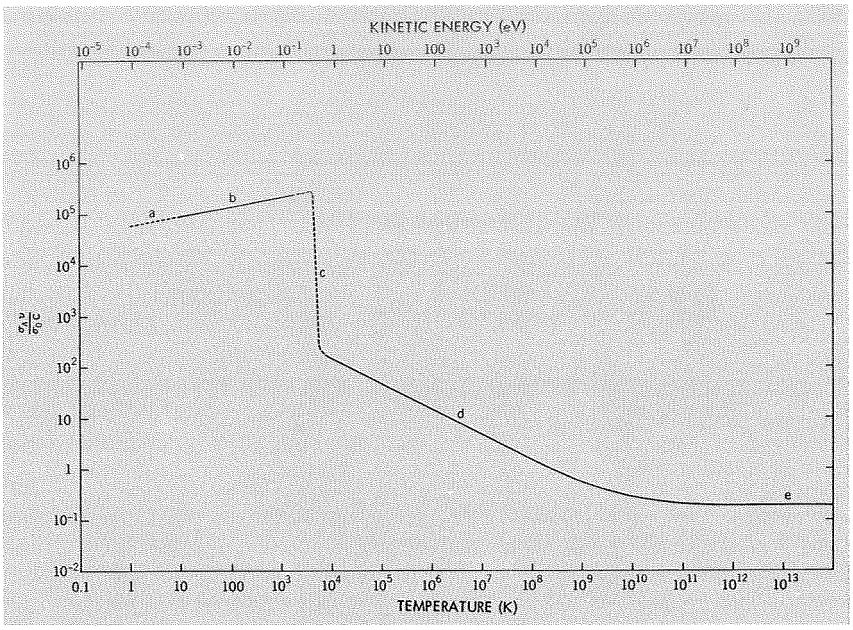

FIGURE 3–2.—Cross section times velocity for hydrogen-antihydrogen annihilation of nucleons given as a sum for the interactions shown in figure 3–1 integrated over a Maxwell-Boltzmann distribution at temperature T and taking ionization into account (Morgan and Hughes, 1970). (*a*) $\sigma_{H+\bar{H}}$ (extrapolated. (*b*) $\sigma_{H+\bar{H}}$ (calculated). (*c*) $\sigma_{H+\bar{H}}$, $\sigma_{p+\bar{H}}$, $\sigma_{p+\bar{H}}$, and $\sigma_{p+\bar{p}}$. multiplied by appropriate factors to take account of fractional ionization. (*d*) $\sigma_{p+\bar{p}}$, taking coulomb attraction into account. (*e*) $\sigma_{p+\bar{p}}$, from high-energy accelerator data.

We will write for all three regions

$$\sigma(E_s|v) = \sigma_i \left(\frac{v}{c}\right)^{-\delta_i} f(E_s) \tag{3–33}$$

where δ_i is the exponent of the power-law velocity dependence of $\sigma(E_s|v)$ as given in equation (3–31) and where, as in previous discussions

$$\int_0^\infty dE_s f(E_s) \equiv 1 \tag{3–34}$$

If we assume that the velocity distribution of the interacting nucleons and antinucleons is thermal and can be represented by the normalized maxwellian distribution

$$f_M(v) = \sqrt{\frac{2}{\pi}} \left(\frac{m}{kT}\right)^{3/2} v^2 \exp\left(-\frac{mv^2}{2kT}\right) \tag{3–35}$$

at some given temperature T; and in addition, if we define a normalized energy spectrum of the γ-radiation in the rest frame of the gas,

$$\zeta_\gamma f(E_{\gamma 0}) \equiv \sum_s \int dE_s f(E_s) \sum_d \zeta_{\gamma d} R_{\gamma d} f_{ds}(E_{\gamma 0}|E_s) \tag{3-36}$$

and smear it out by the distribution function,

$$D(E_\gamma|E_{\gamma 0}) \equiv \left(\frac{mc^2}{2\pi kT}\right)^{1/2} \exp\left[-\frac{mc^2}{2kT}\left(\frac{E_\gamma - E_{\gamma 0}}{E_{\gamma 0}}\right)^2\right] \tag{3-37}$$

to take account of the thermal Doppler broadening of the γ-ray spectrum, we may write equation (3–7) in the form

$$q_{\mathrm{RG}-\overline{\mathrm{RG}}}(E_\gamma, \mathbf{r}) = n_p(\mathbf{r})\, n_{\bar{p}}(\mathbf{r}) \sigma_i c^{\delta_i} \zeta_\gamma \left(\frac{2}{\pi}\right)^{1/2} \left(\frac{m}{kT}\right)^{3/2}$$

$$\times \int dv\, v^{(3-\delta_i)} \exp\left(-\frac{mv^2}{2kT}\right) \int dE_{\gamma 0} D(E_\gamma|E_{\gamma 0}) f(E_{\gamma 0}) \tag{3-38}$$

From the relation

$$\int_0^\infty dv\, v^{(3-\delta_i)} \exp -\frac{mv^2}{2kT} = \frac{1}{2} \Gamma\left(2 - \frac{\delta_i}{2}\right) \left(\frac{2kT}{m}\right)^{\left(2-\frac{\delta_i}{2}\right)} \tag{3-39}$$

where $\Gamma(x)$ is the well-known gamma function

$$\Gamma(x) \equiv \int_0^\infty dy\, y^{x-1} e^{-y} \tag{3-40}$$

which has the property, for integral arguments,

$$\Gamma(N+1) = N! \tag{3-41}$$

equation (3–38) may be further specified to read

$$q_{\mathrm{RG}-\overline{\mathrm{RG}}}(E_\gamma, \mathbf{r}) = n_p(\mathbf{r})\, n_{\bar{p}}(\mathbf{r}) \sigma_i c^{\delta_i} \zeta_\gamma \frac{2}{\pi^{1/2}} \Gamma\left(2 - \frac{\delta_i}{2}\right)$$

$$\times \left(\frac{2kT}{m}\right)^{1/2(1-\delta_i)} \int dE_{\gamma 0}\, D(E_\gamma|E_{\gamma 0}) f(E_{\gamma 0}) \tag{3-42}$$

Let us now utilize equation (3–42) to specifically discuss the tempera-

ture regions I, II, and III defined earlier. In region I, $\delta_{\mathrm{I}} = 1$, and therefore, from equation (3–7),

$$\int dv f(v) v \sigma_{\mathrm{I}} c v^{-1} = \sigma_{\mathrm{I}} c \int dv f(v) v \cdot v^{-1} = \sigma_{\mathrm{I}} c \int dv f(v)$$

$$= \sigma_{\mathrm{I}} c \tag{3–43}$$

since $\int dv f(v) \equiv 1$ by definition.

We therefore find that in region I,

$$q_{\mathrm{RG}-\overline{\mathrm{RG}}}(E_\gamma, \mathbf{r}) = n_p(\mathbf{r}) n_{\bar{p}}(\mathbf{r}) \sigma_{\mathrm{I}} c \zeta_\gamma \int dE_{\gamma 0} D(E_\gamma | E_{\gamma 0}) f(E_{\gamma 0})$$

$$\text{for } 10^{11}\ \mathrm{K} \lesssim T \lesssim 10^{13}\ \mathrm{K} \tag{3–44}$$

In temperature regions II and III, we cannot make the simplification given by equation (3–43); however, we can make a different simplification. In these temperature regions, $\beta \ll 1$, and Doppler broadening due to thermal effects provides only a negligible distortion on the γ-ray spectrum. Thus, in these temperature regions, we may write

$$D(E_\gamma | E_{\gamma 0}) \simeq \delta(E_\gamma - E_{\gamma 0}) \qquad (\beta \ll 1) \tag{3–45}$$

and therefore

$$\int dE_{\gamma 0} D(E_\gamma | E_{\gamma 0}) f(E_{\gamma 0}) \simeq f(E_\gamma) \tag{3–46}$$

In region II, $\delta_{\mathrm{II}} = 2$, and by reducing equation (3–42) and making use of the approximation (3–46), we obtain

$$q_{\mathrm{RG}-\overline{\mathrm{RG}}}(E_\gamma, \mathbf{r}) = n_p(\mathbf{r}) n_{\bar{p}}(\mathbf{r}) \sigma_{\mathrm{II}} c \zeta_\gamma \left(\frac{2mc^2}{\pi kT}\right)^{1/2} f(E_\gamma)$$

$$\text{for } 10^{4}\ \mathrm{K} \lesssim T \lesssim 10^{11}\ \mathrm{K} \tag{3–47}$$

In region III, $\delta_{\mathrm{III}} = 0.64$, and again reducing equation (3–42) and using the approximation (3–46), we find

$$q_{\mathrm{RG}-\overline{\mathrm{RG}}}(E_\gamma, \mathbf{r}) = n_p(\mathbf{r}) n_{\bar{p}}(\mathbf{r}) \sigma_{\mathrm{III}} c \zeta_\gamma \left[\frac{2}{\pi^{1/2}} \Gamma(1.68) \left(\frac{2kT}{mc^2}\right)^{0.18}\right] f(E_\gamma)$$

$$\text{for } 10\ \mathrm{K} \lesssim T \lesssim 10^{4}\ \mathrm{K} \tag{3–48}$$

We will consider more detailed applications of equations (3–44), (3–47), and (3–48) in a later chapter when we consider cosmological

formulations of these equations. However, it might be useful at this point to consider a simplified numerical example of these equations.

Present theoretical conceptions, based on recent empirical studies, indicate that the intergalactic medium is probably a very tenuous ionized gas with an average density of 10^{-7} to 10^{-5} atom per cubic centimeter at a temperature between 10^4 and 10^6 K, which places it in our temperature region II. It is found experimentally that approximately three γ-rays of energy greater than 100 MeV are produced for each p–$\bar{p}$ annihilation (i.e., $\zeta_\gamma = 3$). From equations (3–8), (3–9) and (3–47), and by taking $T = 10^6$ K, we find

$$I_{\mathrm{RG}-\overline{\mathrm{RG}}}(E_\gamma > 100\ \mathrm{MeV}) \simeq \frac{3B}{4\pi}\,\sigma_{\mathrm{II}}\,c\left(\frac{2mc^2}{\pi kT}\right)^{1/2}$$
$$\simeq 4.1 \times 10^{-14} B\ (\mathrm{cm^{-2}\text{-}s^{-1}\text{-}sr^{-1}}) \qquad (3\text{–}49)$$

Recent measurements (Clark, Garmire, and Kraushaar, 1968) have indicated that the isotropic flux of cosmic γ-rays in this energy region is $\lesssim 10^{-4}$ $\mathrm{cm^{-2}\text{-}s^{-1}\text{-}sr^{-1}}$. This places an upper limit on the emission measure B:

$$B \leqslant 2.4 \times 10^9 \qquad \mathrm{cm^{-5}} \qquad (3\text{–}50)$$

and, from equation (3–8), indicates that by dividing by the visible radius of the universe R_u,

$$\langle n_p n_{\bar{p}} \rangle = \frac{B}{R_u} \lesssim 2.4 \times 10^{-19} \qquad \mathrm{cm^{-6}} \qquad (3\text{–}51)$$

Thus, if $n_p \gtrsim 10^{-7}$ $\mathrm{cm^{-3}}$, the mean density of antimatter in intergalactic space is $\lesssim 2 \times 10^{-12}$ particles per cubic centimeter.

We will now go on to calculate the energy spectrum $f(E_\gamma)$.

3–4 MESON PRODUCTION AND THE STATISTICAL MODEL OF MATSUDA

In considering the production of mesons from p–$\bar{p}$ annihilation, we refer to the simple statistical model of Matsuda (1966) and the data of the Columbia University group presented in the Matsuda reference.

The Matsuda model assumes that shortly after annihilation the total energy of the p–$\bar{p}$ system (equal to $2m_p$) is distributed in an interaction volume Ω and that the system reaches thermal equilibrium. Since in the

annihilation the wave packets of the two particles completely overlap in an S state, then for

$$\Omega \simeq \left(\frac{\hbar}{m_\pi c}\right)^3$$

$$n_s \simeq \frac{\langle \zeta \rangle_{\text{expt}}}{\Omega} \tag{3-52}$$

$$\sigma \simeq \left(\frac{\hbar}{m_\pi c}\right)^2$$

(where n_s is the density of secondary particles produced) we find that the mean free path of the meson produced, l_{mfp}, is

$$l_{\text{mfp}} = \frac{1}{n_s \sigma} \simeq 10^{-1} \lambda_{\text{st}} \tag{3-53}$$

for an experimentally observed average number of mesons produced, ζ_{expt}, where λ_{st} is the distance traveled by the meson during the strong interaction in time $t_{\text{st}} = \lambda_{\text{st}} c^{-1} \simeq 10^{-23}$ s. Thus, we find that there is enough time available for the created mesons to collide with each other and reach thermal equilibrium before they leave the interaction volume Ω. Matsuda then assumes that there exists a quantized energy level $\epsilon_\tau > 0$ for each type of meson ($\tau = \pi, \rho, \omega, \eta, K, K^*$, etc.) produced in the annihilation. The whole system reaches a thermal equilibrium given by the parameter $\Phi = 1/kT$ at temperature T, which is therefore the same for each nonstrange boson (type $\sigma = \pi$, ρ, ω, η, etc.) or strange meson pair (type $\nu = K\bar{K}$, $K^*\bar{K}^*$, etc.). We designate the statistical weights by

$$g_\tau = (2S_\tau + 1)(2T_\tau + 1) \tag{3-54}$$

T_τ being the isospin of particle τ. Because the created mesons are bosons, we obtain

$$\langle \zeta_\tau \rangle = \frac{g_\tau}{e^{\Phi \epsilon_\tau} - 1} \tag{3-55}$$

Matsuda then introduces the chemical potential parameter ϵ_0 associated with the production of each particle and related to the observed average energy $\langle E_\tau \rangle$ of each particle through the relation

$$\epsilon_\tau = \langle E_\tau \rangle - \epsilon_0 \tag{3-56}$$

which must satisfy the condition

$$\epsilon_0 < \langle E_\tau \rangle \tag{3-57}$$

so that for nonstrange mesons equation (3–55) becomes

$$\langle \zeta_\sigma \rangle = \frac{g_\sigma}{\exp\left[\Phi(\langle E_\sigma \rangle - \epsilon_0)\right] - 1} \tag{3–58}$$

For pairs of strange mesons, equation (3–55) becomes

$$\langle \zeta_\nu \rangle = \frac{g_\nu}{\exp\left[\Phi(\langle E_\nu \rangle - 2\epsilon_0)\right] - 1} \tag{3–59}$$

since the formation of each meson involves energy ϵ_0.

The observed average energies of the various mesons produced in p–$\bar{p}$ annihilations at rest are listed by Matsuda and given here in table 3–2. We find that by specifying

$$\frac{1}{\Phi} = 150 \text{ MeV}$$

and (3–60)

$$\epsilon_0 = 295 \text{ MeV}$$

we obtain excellent agreement with the experimental production rate, as shown in table 3–2. The total average number of produced particles calculated from equations (3–58) and (3–59) is

$$\langle \zeta_{\text{Total}} \rangle = \sum_\sigma \langle \zeta_\sigma \rangle + \sum_\nu 2\langle \zeta_\nu \rangle = 4.37 \tag{3–61}$$

TABLE 3–2.—*Average Energies and Production Rates for Various Particles Produced in* p–$\bar{\text{p}}$ *Annihilations at Rest*

[Matsuda, 1966]

τ, particle or pair	Average energy, MeV	Calculated production rate	Experimental production rate
π	380	3.96	3.94 ± 0.33
ρ	850	2.3×10^{-1}	$(2.5 \pm 0.6) \times 10^{-1}$
ω	940	4.2×10^{-2}	$(4.5 \pm 0.7) \times 10^{-2}$
η	860	2.4×10^{-2}	$(1.4 \pm 0.5) \times 10^{-2}$
$K\bar{K}$	$(K)660$	3.1×10^{-2}	$(3.3 \pm 1.6) \times 10^{-2}$
$K\bar{K}^*, \bar{K}K^*$		20.6×10^{-3}	$(8.8 \pm 1.8) \times 10^{-3}$
$K^*\bar{K}^*$	$(K^*)980$	3.8×10^{-3}	$(3.9 \pm 0.7) \times 10^{-3}$

The value given by the experimental results is

$$\langle \zeta_{\text{Total}} \rangle_{\text{expt}} = 4.34 \tag{3-62}$$

which also agrees well with the calculation.

Both the experimental data and the simple statistical model of Matsuda indicate that in $p-\bar{p}$ annihilations at rest, ρ-meson production is an order of magnitude less important than pion production and that production of other mesons is at least two orders of magnitude less frequent than pion production. Table 3–3 shows the decay schemes of these mesons that lead to final-state γ-rays and other relevant data. Table 3–4 shows some recent data on meson production indicating that about 20 percent of the γ-rays produced arise through nonpionic meson production. The largest nonpion contribution to the γ-ray spectrum is due to the ρ-meson decay schemes

$$\begin{array}{l} \rho^{\pm} \rightarrow \pi^{\pm} + \pi^0 \\ \qquad\quad \hookrightarrow \gamma + \gamma \end{array} \tag{3-63}$$

The ρ meson is an isospin triplet ($T=1$) constructed from two pions,

TABLE 3–3.—*Decay Modes, Branching Ratios, and γ-Ray Multiplicities for Various Particles Produced in* p–$\bar{\text{p}}$ *Annihilations*

Decay mode	Branching ratio, R	$\zeta_\gamma R$
$\rho^{\pm} \rightarrow \pi^{\pm} + \pi^0$	~ 1.00	2.0
$\omega \rightarrow \pi^+ + \pi^- + \pi^0$	.89	1.78
$\rightarrow \pi^0 + \gamma$	.10	.30
$\eta \rightarrow \gamma + \gamma$	.386	.78
$\rightarrow 3\pi^0$ or $\pi^0 + 2\gamma$	.308	1.5
$\rightarrow \pi^+ + \pi^- + \pi^0$	.250	.5
$\rightarrow \pi^+ + \pi^- + \gamma$	.055	.05
$K^{\pm} \rightarrow \pi^{\pm} + \pi^0$ [a]	.215	.43
K_0 $K_1^0 \rightarrow \pi^0 + \pi^0$	.155	.62
K_0 $K_2^0 \rightarrow \pi^0 + \pi^0 + \pi^0$	.133	.80
K_0 $K_2^0 \rightarrow \pi^+ + \pi^- + \pi^0$	.067	.1
$K^* \rightarrow K + \pi$	—	—

[a] Other γ-ray-producing decay modes have negligible branching ratios.

TABLE 3–4.—*Production Rates for Various Meson-Producing Channels in* $p-\bar{p}$ *Annihilations at Rest*

[From Baltay et al., 1964]

Channel	Rate, %	ζ_γ	$\zeta_\gamma R$
$\rho^0\pi^0$	1.4 ± 0.2	2	2.8
$\rho^\pm\pi^\mp$	2.9 ± 0.4	2	5.8
$\rho^0\pi^+\pi^-$ [a]	$5.8\ ^{+0.3}_{-1.3}$	0	0
$\rho^0\rho^0$	0.4 ± 0.3	0	0
$\rho^0\pi^+\pi^-\pi^0$	7.3 ± 1.7	2	14.6
$\rho^\pm\pi^\mp\pi^+\pi^-$	6.4 ± 1.8	2	12.8
$\omega^0\pi^+\pi^-$ [a]	3.8 ± 0.4	2	7.6
$\eta^0\pi^+\pi^-$ [a]	1.2 ± 0.3	~ 2.6	3.1
$\omega^0\rho^0$	0.7 ± 0.3	2	—
$\eta^0\rho^0$	0.22 ± 0.17	~ 2.6	—

[a] Includes cases where $\pi^+\pi^-$ were from ρ^0 decay.

each having $T=1$. Evaluation of the Clebsch-Gordon coefficients for this construction yields

$$|\rho^+\rangle = \frac{1}{\sqrt{2}}\left(|\pi^+\rangle|\pi^0\rangle - |\pi^0\rangle|\pi^+\rangle\right)$$

$$|\rho^0\rangle = \frac{1}{\sqrt{2}}\left(|\pi^+\rangle|\pi^-\rangle - |\pi^-\rangle|\pi^+\rangle\right) \tag{3–64}$$

$$|\rho^-\rangle = \frac{1}{\sqrt{2}}\left(|\pi^0\rangle|\pi^-\rangle - |\pi^-\rangle|\pi^0\rangle\right)$$

Since the ρ^0 construction does not contain any $|\pi^0\rangle|\pi^0\rangle$ terms,

$$|\langle\pi^0\pi^0|\rho^0\rangle|^2 = 0 \tag{3–65}$$

and, therefore,

$$\rho^0 \not\to \pi^0 + \pi^0 \tag{3–66}$$

Gamma rays from $\rho^\pm$ decay (reaction (3–63)) possess an average energy of 210 MeV, not much different from the 190-MeV average energy given to γ-rays from the directly produced pions that are an order of magnitude more frequent. Because other mesons are produced even less frequently than the ρ mesons, we can conclude that mesons other than pions have a negligible effect on the total γ-ray spectrum from $p-\bar{p}$ annihilation.

3–5 SELECTION RULES

If we assume that the large majority of γ-rays from RG–$\overline{\text{RG}}$ interactions arise through π^0 decay (as was shown in the previous section), equation (3–36) reduces to

$$f(E_\gamma) = \int_{E\gamma+(m_\pi^2/4E\gamma)}^{\infty} dE_\pi \frac{f_A(E_\pi)}{(E_\pi^2 - m_\pi^2)^{1/2}} \tag{3–67}$$

as we showed in our derivation of equation (1–100).

The process

$$p + \bar{p} \rightarrow \pi^0 \tag{3–68}$$

is, of course, forbidden by conservation of momentum. The process

$$p + \bar{p} \rightarrow \pi^0 + \pi^0 \tag{3–69}$$

is also forbidden since p–$\bar{p}$ annihilations at rest occur predominantly from the S states of the p–$\bar{p}$ system.

The selection rule that forbids reaction (3–69) follows from conservation of G conjugation parity.

The process of G conjugation is an extension of charge (C) conjugation, which holds for neutral as well as charged particles. It is defined as

$$G = Ce^{i\pi T_2} \tag{3–70}$$

where C is the charge-conjugation operator and T_2 is the second component of the isospin vector. From (3–70) we can show the commutation relation

$$[\mathbf{T}, G] = 0 \tag{3–71}$$

Thus, we may describe particle states as simultaneous eigenstates of both G and T.

It can be shown (Sakurai, 1964) that systems having baryon number 0 are in an eigenstate of G. The p–$\bar{p}$ system is just such a system. For this system

$$G = (-1)^{L+S+T} \tag{3–72}$$

where L, S, and T are the orbital, spin, and isospin quantum numbers of the state, respectively.

In a state consisting of a single pion, $L = 0, S = 0, T = 1$, and, therefore, $G = -1$. In a final state consisting of ζ_π pions, G is given by

$$G = (-1)^{\zeta_\pi} \tag{3–73}$$

The selection rules (3–72) and (3–73) indicate that for an S-state annihilation ($L=0$), the final state consisting of two neutral pions is strictly forbidden (Lee and Yang, 1956).

Therefore, the extremum γ-ray energies that we would expect from this decay would result from interactions of the type

$$p+\bar{p}\rightarrow \pi^+ + \pi^- + \pi^0 \tag{3–74}$$

resulting in pions with the given maximum energy

$$\begin{aligned} E_{\pi^0,\,\max} &= \frac{1}{2(2m_p)}\left[(2m_p)^2 + m_{\pi^0}^2 - (2m_{\pi^\pm})^2\right] \\ &= m_p - \frac{3}{4}\frac{m_\pi^2}{m_p} \simeq 923 \text{ MeV} \end{aligned} \tag{3–75}$$

Thus, the annihilation γ-rays are limited to the energy region

$$\tfrac{1}{2}\left[E_{\pi^0,\,\min} - (E_{\pi^0,\,\max}^2 - m_\pi^2)^{1/2}\right] \leq E_\gamma \leq \tfrac{1}{2}\left[E_{\pi^0,\,\max} + (E_{\pi^0,\,\max}^2 - m_\pi^2)^{1/2}\right] \tag{3–76}$$

or 5 MeV $\leq E_\gamma \leq$ 919 MeV.

The process

$$p+\bar{p}\rightarrow \gamma+\gamma \tag{3–77}$$

may also occur; but this process, involving the electromagnetic emission (em) of two photons, is of the order

$$\sigma_{\text{em}} = \alpha^2 \sigma_{A,\,\text{strong}} \simeq \frac{2.6\times 10^{-30}\ \text{cm}^2}{\beta} \tag{3–78}$$

and therefore this process may be neglected as a significant contribution to γ-ray production.

3–6 THE GAMMA-RAY SPECTRUM FROM PROTON-ANTIPROTON ANNIHILATIONS AT REST

As we showed in the previous section, we can neglect the contribution from the decay of mesons other than neutral pions in calculations of the γ-ray spectrum from p–$\bar{p}$ annihilations at rest. The normalized γ-ray spectrum was calculated numerically from the relation (3–68) by the author, with the normalized distribution function $f_A(E_\pi)$ taken from the calculations of Maksimenko (1958), based on the statistical theory of multiple particle production.

The resultant spectrum, up to 750 MeV, is shown in figure 3–3. Frye and Smith (1966) have recently calculated the γ-ray spectrum from p–$\bar{p}$

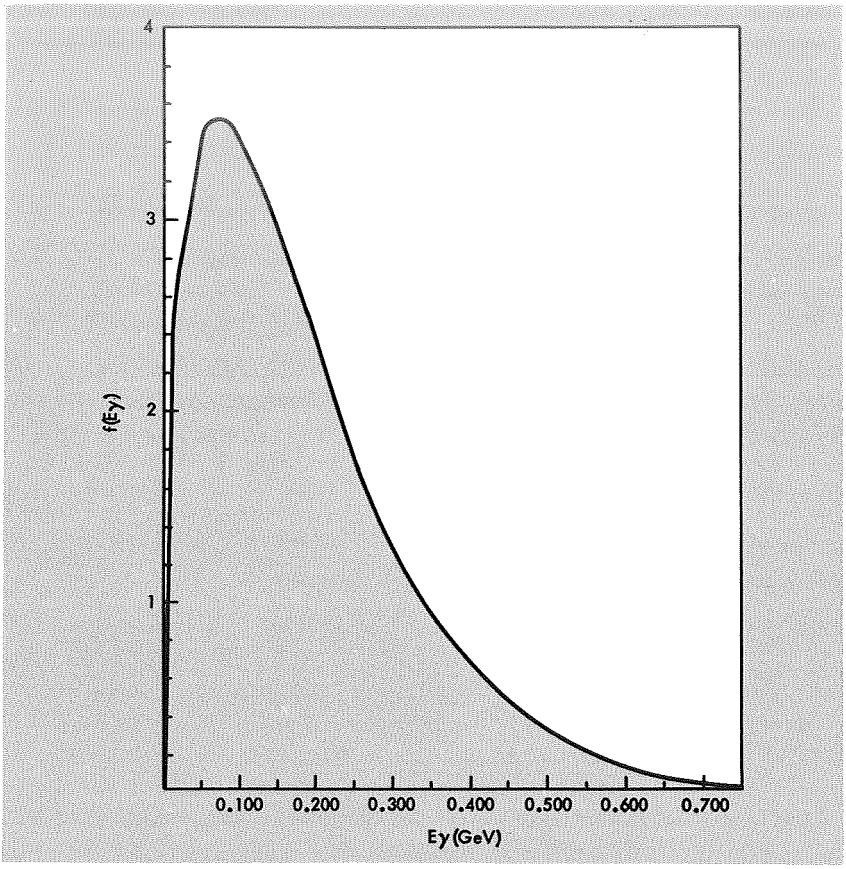

FIGURE 3–3.—Normalized γ-ray spectrum from p–$\bar{p}$ annihilation.

annihilation up to 500 MeV, based on recent measurements of charged pions from p–$\bar{p}$ annihilation by the Columbia University group. The excellent agreement between the results of figure 3–3 and the calculations of Frye and Smith not only serves as a mutual check on the calculations but also supports our previous conclusion that mesons other than pions have a negligible effect on the total γ-ray spectrum from p–$\bar{p}$ annihilation at rest.

The absolute magnitude of the γ-ray spectrum from p–$\bar{p}$ annihilation at rest is obtained from equation (3–44), (3–47), or (3–48), depending upon the temperature region involved.

3–7 PROTON-ANTIPROTON ANNIHILATIONS IN FLIGHT

We now turn our attention to RG–$\overline{\text{CR}}$ interactions. Here, because of limitations in the data, as well as kinematic and dynamic similarities that

would make the γ-ray spectra from such interactions difficult to distinguish from the γ-ray spectra of the much more prevalent RG–CR interactions, we will present only a qualitative treatment.

An excellent review article on high-energy interactions of antiprotons in hydrogen has been presented by Baltay et al. (1964). For high-energy p–$\bar{p}$ interactions, annihilations of the types

$$p + \bar{p} \rightarrow p + \bar{p} + \text{bosons} \tag{3–79}$$

$$p + \bar{p} \rightarrow \begin{cases} N + \bar{N}^* + \text{bosons} \\ N^* + \bar{N} + \text{bosons} \\ N^* + \bar{N}^* + \text{bosons} \end{cases} \tag{3–80}$$

and

$$p + \bar{p} \rightarrow \begin{cases} Y + \bar{Y} \\ Y + \bar{Y}^* + \text{bosons} \\ Y^* + \bar{Y} + \text{bosons} \\ Y^* + \bar{Y}^* + \text{bosons} \end{cases} \tag{3–81}$$

may occur, as well as annihilations of the type previously considered.

Reactions of the type given by equation (3–80) seem to occur frequently and to be of a similar nature as p–p interactions. For example (Ferbel et al., 1962, and Ferbel et al., 1965), p–$\bar{p}$ interactions in the 3- to 4-GeV/c range lead to strong production of the $\Delta(1.238)$ isobar, while at 7 GeV/c no single resonance seems to dominate. The angular distribution of the outgoing baryons is strongly peaked in the forward and backward directions in the collision cms. All these facts hold true for the p–p interactions as we will discuss in detail in chapter 6. In the energy range where production of the $\Delta(1.238)$ isobar predominates, production of neutral pions occurs at roughly the same rate in both p–p and p–$\bar{p}$ interactions, as indicated in table 3–5 (Baltay et al., 1964).

This fact, too, strongly highlights the similarity between p–p and nonannihilation p–$\bar{p}$ interactions at similar energies. Thus, in the 3- to

TABLE 3–5.—*Cross Sections for Inelastic Single Neutral-Pion Production in* p–$\bar{\text{p}}$ *Interactions as a Function of Incident Momentum*

Reaction	Collision momentum, GeV/c	Cross section, mb
$\bar{p} + p \rightarrow \bar{p} + p + \pi^0$	3.25	2.3 ± 0.5
$p + p \rightarrow p + p + \pi^0$	3.67	2.9 ± 0.3

4-GeV/c range, neutral (and charged) pion production is dominated by the channel

$$\begin{array}{ccc} & \Delta+\bar{N} & \\ \nearrow & & \searrow \\ p+\bar{p} & & N+\bar{N}+\pi^0 \\ \searrow & & \nearrow \\ & \bar{\Delta}+N & \end{array} \qquad (3\text{–}82)$$

It may therefore be assumed that the nonannihilation RG–$\overline{\text{CR}}$ (or CR–$\overline{\text{RG}}$) interactions will lead to γ-ray spectra with the same characteristics as those from high-energy p–p interactions. (See chs. 5 and 6.) Experiments also show that in p–$\bar{p}$ interactions between 1.6 and 7.0 GeV/c (Böckmann et al., 1966), nonannihilation production of pions increases with respect to annihilation production. At 5.7 GeV/c, the cross sections for the two processes are comparable (and also are comparable to the cross section for inelastic p–p interactions).

Böckmann et al. (1966) find these values for the cross sections at 5.7 GeV/c:

$$\begin{array}{ll} p+\bar{p}\rightarrow p+\bar{p}+\text{bosons (inelastic)} & 24.8\pm 2.0 \text{ mb} \\ p+\bar{p}\rightarrow \text{bosons (annihilation)} & 22.5\pm 2.0 \text{ mb} \end{array} \qquad (3\text{–}83)$$

The pion multiplicity in annihilation interactions rises slowly with energy, as shown in table 3–6.

The cross sections in tables 3–7 and 3–8 are comparable in magnitude to those given in chapter 5 for hyperon production in p–p interactions. As in p–p interactions, these cross sections are small relative to pion-production cross sections, but increase with energy. The outgoing hyperons are observed to be emitted strongly in the forward and backward directions, as in the case of p–p interactions. Also, in interactions involving final-state Y- and π-production, resonances (strange isobars) of the type

$$Y^*\rightarrow Y+\pi \qquad (3\text{–}84)$$

are commonly produced.

TABLE 3–6.—*Average Pion Multiplicity in Annihilation Interactions as a Function of Incident Momentum*

Momentum, GeV/c	Multiplicity	Reference
0	~ 4.3	Matsuda (1966)
3.25	~ 6.0	Baltay et al. (1964)
5.7	~ 7.3	Böckmann et al. (1966)

TABLE 3–7.—*Cross Sections for Hyperon-Antihyperon Production in* $p-\bar{p}$ *Interactions*

Final state	Cross section, μb	
	3.25 GeV/c	3.69 GeV/c
$\Lambda\bar{\Lambda}$	87 ± 13	94 ± 14
$\Lambda\bar{\Sigma}^0$, $\bar{\Lambda}\Sigma^0$	56 ± 11	76 ± 14
$\Sigma^+\bar{\Sigma}^-$, $\Sigma^-\Sigma^+$	38 ± 11	56 ± 14
$\Xi^-\Xi^+$	4 [a]	5 [a]
$\Lambda\bar{\Lambda} + n\pi^0$, $\Lambda\bar{\Sigma}^0 + n\pi^0$, $\bar{\Lambda}\Sigma^0 + n\pi^0$	102 ± 39	122 ± 43
$\Lambda\bar{\Lambda}\pi^+\pi^-$	15 ± 6	30 ± 9
$\Sigma^\pm\bar{\Lambda}\pi^\mp$, $\bar{\Sigma}^\pm\Lambda\pi^\mp$	51 ± 18	143 ± 45
$\Sigma^\pm\bar{\Sigma}^\mp\pi^0$	7 ± 5	28 ± 19
$KN(\bar{\Lambda}$ or $\bar{\Sigma})$, $K\bar{N}(\Lambda$ or $\Sigma)$	24 ± 10	41 ± 14
Total antihyperon production	438 ± 52	710 ± 78

[a] Based on one event at each energy.

TABLE 3–8.—*Cross Sections for the Reaction* $p + \bar{p} \rightarrow \Lambda + \bar{\Lambda}$ *as a Function of Incident Momentum*

Momentum, GeV/c	Cross section, μb	Reference
1.61	57 ± 18	Button et al. (1961)
3.25	87 ± 13	Baltay et al. (1964)
3.69	94 ± 14	Baltay et al. (1964)

We can summarize the findings for high-energy $p-\bar{p}$ interactions as follows:

(1) There are two distinct types of pion-production processes that may be considered: (*a*) annihilations and (*b*) inelastic pion production without annihilation.
(2) The ratio of occurrence of process (*b*) relative to process (*a*) increases with increasing energy between 1.6 and 7.0 GeV/c and is approximately 1 at 5.7 GeV/c.
(3) Inelastic interactions (without annihilation) are very similar to $p-p$ interactions and exhibit similar resonance production and forward-backward peaking.

(4) Strange particles are produced in similar quantities in both inelastic $p-p$ and $p-\bar{p}$ interactions.

For these reasons, we may assume that

(1) An "isobar-plus-fireball" model, similar to that discussed in chapter 5 may be applicable to high-energy $p-\bar{p}$ interactions. In this case, annihilation interactions may be included as an added contribution to the fireball component.

(2) At high energies ($E_\gamma > 5$ GeV) there is at present no reason to assume that the characteristics of the γ-ray spectrum from $p-\bar{p}$ interactions will differ from those of the γ-ray spectrum from $p-p$ interactions.